Molecular Dynamics Study of Ultra-Long Chain Fatty Acid in Lipid Bilayer

Kazutomo KAWAGUCHI[1], and Hiroshi NOGUCHI[2]
[1]*Institute of Science and Engineering, Kanazawa University*
Kanazawa, Ishikawa 920-1192
[2]*Institute for Solid State Physics, University of Tokyo*
Kashiwa-no-ha, Kashiwa, Chiba 277-8581

Abstract

Although ultra-long-chain fatty acids (ULCFAs) exist in biomembranes in certain types of tissues, their biological roles remain unknown. In this report, we review our recent study on the molecular conformation of ULCFAs in lipid bilayers using molecular dynamics simulations. Their long chains exhibit characteristic fluctuations between elongated, L-shaped, and turned conformations. The ratios of these conformations are changed in response to the lipid-density differences between upper and lower leaflets. This response is faster than the flip–flop of cholesterols.

1 Introduction

Biological membranes consist of various types of lipids and proteins [1]. Phospholipids are the most abundant lipids in biological membranes and have a polar head group and two hydrocarbon tails (fatty acids). Phospholipids are biosynthesized by a combination of a polar head group and two hydrocarbon tails and have a range of structural and functional roles in biological cells [2, 3]. Each tail typically contains between 14 and 22 carbon atoms. Fatty acids containing more than 22 carbons are called very-long-chain fatty acids (VLCFAs). Moreover, much longer chains containing more than 32 carbons were found at the sn-1 position of phosphatidylcholine (PC) in photoreceptors, fibroblasts, and keratinocytes [4, 5, 6]. These fatty acids are called ultra-long-chain fatty acids (ULCFAs). It is considered that ULCFAs are stored as a precursor of bioactive lipid mediators [7] and derivatives of C32:6 and C34:6 are neuroprotective in retina [8]. However, the physicochemical properties of ULCFAs with respect to their structures and the biological roles of ULCFA-containing phospholipids are still unclear.

Molecular simulations have been widely applied to study lipid membranes [9, 10, 11, 12, 13]. All-atom molecular dynamics (MD) simulations for VLCFAs, in which the tail length of the sn-1 chain is maximally 24, have also been performed by a few groups [14, 15, 16, 17, 18]. It has been shown that the long hydrocarbon chain is slightly interdigitated into the opposite leaflet [14, 16, 17]. However, ULCFAs had not been simulated yet. To examine the effects of ultra-long chains, we have conducted all-atom MD simulations for ULCFAs [19, 20]. Our study revealed that the longer chains of ULCFAs have more strongly interacted with the opposite leaflet than those of VLCFAs. The ultra-long sn-1 chain of ULCFAs takes elongated, L-shaped, and turned conformations in lipid bilayers and that these conformational change can reduce the lipid-density difference between upper and lower leaflets.

Three types of ULCFAs are used in this

study. The chain length and number of unsaturated bonds are varied. Lipid molecules composing Host bilayer membranes consist of single or two types of phospholipids. Moreover, cholesterols (CHOLs) are embedded in the bilayer membrane to examine the effect of the flip–flop of cholesterols.

2 Methods

2.1 ULCFAs

The molecular structures of ULCFAs used in this study are shown in Fig. 1. Dotriacontahexaenoic acid containing phosphatidylcholine (dTSPC, C32:6-C18:0), which has an ultra-long chain of 32 carbons with six double bonds at the sn-1 position [Fig. 1(a)]. Hexacosatetraenoic acid containing phosphatidylcholine (HSPC, C26:4-C18:0), which has a very-long chain of 26 carbons with four double bonds at the sn-1 position [Fig. 1(b)]. Lacceroic acid containing phosphatidylcholine (LSPC, C32:0-C18:0), which has an ultra-long chain of 32 carbons with no double bonds at the sn-1 position [Fig. 1(c)]. All of the ULCFAs have a stearoyl chain at the sn-2 position. HSPC is constructed by truncating the long hydrocarbon chain of dTSPC at C26, and LSPC is constructed by the saturation of the long hydrocarbon chain of dTSPC. A single ULCFA molecule (dTSPC, HSPC, or LSPC) was inserted into the lipid bilayers described in the next section.

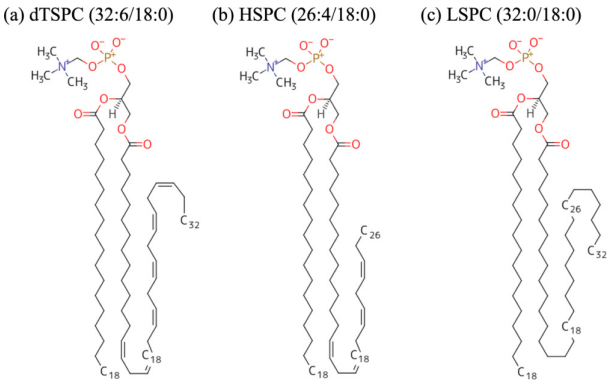

Figure 1: Molecular structures of ULCFAs. (a) dTSPC (C32:6-C18:0), (b) HSPC (C26:4-C18:0), and (c) LSPC (C32:0-C18:0).

2.2 Lipid Bilayer

The molecular structures of lipids composing bilayer membranes are shown in Fig. 2. Distearoyl phosphatidylcholine (DSPC, C18:0-C18:0) contains two saturated stearoyl chains. Stearoyl-DHA phosphatidylcholine (SDPC, C18:0-C22:6) contains a steroyl chain and a docosahexaenoyl chain with six double bonds at the sn-1 and sn-2 positions, respectively. Stearoyl-oleoyl phosphatidylcholine (SOPC, C18:0-C18:1) contains a steroyl chain and an oleoyl chain with a double bond at the sn-1 and sn-2 positions, respectively.

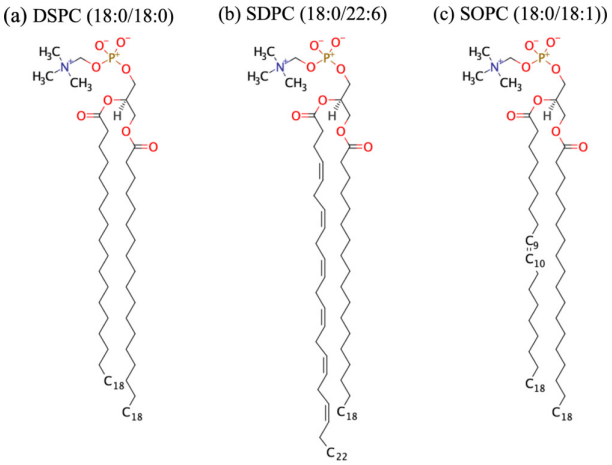

Figure 2: Molecular structures of lipids composing bilayer membranes. (a) DSPC (C18:0-C18:0), (b) SDPC (C18:0-C22:6), and (c) SOPC (C18:0-C18:1).

We considered three types of host lipid bilayers for embedding a single ULCFA molecule: (1) single-component bilayers. (2) asymmetric-component bilayers, in which each leaflet is composed of a single type of phospholipids. (3) two-component bilayers composed of a single type of phospholipids and cholesterols.

(1) DSPC, SDPC, and SOPC were used for single-component host bilayers and dTSPC was used as ULCFA. A membrane bilayer consisting of 100 lipid molecules per leaflet was prepared for each membrane system. The membrane was connected by its periodic images in the xy plane under the periodic boundary conditions. A single lipid molecule in the upper leaflet was replaced by a single dTSPC molecule for each single-component bilayer, in order to examine the influence of the difference between upper and lower leaflets on the long sn-1 chain of dTSPC (see Table 1). Ten lipid molecules in the upper (lower) leaflet were removed in the '189u' ('189l') system. Four lipid molecules in the upper (lower) leaflet were removed in the '195u' ('195l') system. Two lipid molecules in the upper (lower) leaflet were removed in the '197u' ('197l') system. Labels 189, 195, and 197 represent the total number of the host lipid molecules. The number of water molecules per lipid was fixed at 50 in all cases. The lipids do not flip–flop to the opposite leaflets on a simulation time scale (the flip–flop time is typically hours or days [21]). The difference of the lipid numbers between the two leaflets results in the deviation of the lipid density from a stable value even under zero surface tension, as described by an area-difference-elasticity model [22, 23]. Thus, the lipids in the leaflet with higher density are more compressed, although a flat membrane connected by the periodic boundary does not bend because of the symmetry. The DSPC/dTSPC and SDPC/dTSPC mixtures were equilibrated for 200 ns, which was followed by 800-ns production runs at 343 K. to avoid the gel phase of DSPC and SDPC. The SOPC/dTSPC mixtures were equilibrated for 400 ns, which was followed by 1.6 μs-production runs at 303 K.

Table 1: Numbers of phospholipids in single-component host bilayers. A single dTSPC molecule was embedded.

Model	Upper leaflet	Lower leaflet
DS189u	89 DSPCs	100 DSPCs
DS189l	99 DSPCs	90 DSPCs
DS197u	97 DSPCs	100 DSPCs
DS197l	99 DSPCs	98 DSPCs
SD189u	89 SDPCs	100 SDPCs
SD189l	99 SDPCs	90 SDPCs
SD197u	97 SDPCs	100 SDPCs
SD197l	99 SDPCs	98 SDPCs
SO189u	89 SOPCs	100 SOPCs
SO189l	99 SOPCs	90 SOPCs
SO195u	95 SOPCs	100 SOPCs
SO195l	99 SOPCs	96 SOPCs
SO197u	97 SOPCs	100 SOPCs
SO197l	99 SOPCs	98 SOPCs

Table 2: Numbers of phospholipids in asymmetric-component host bilayer membranes. Three types of ULCFAs were embedded in the bilayers.

Membrane	Upper leaflet	Lower leaflet
DS89-SD100	89 DSPCs	100 SDPCs
DS99-SD90	99 DSPCs	90 SDPCs
DS99-SD98	99 DSPCs	98 SDPCs
SD89-DS100	89 SDPCs	100 DSPCs
SD99-DS90	99 SDPCs	90 DSPCs
SD99-DS98	99 SDPCs	98 DSPCs

(2) A DSPC/SDPC mixture asymmetric bilayer was used as a host lipid bilayer. We prepared six types of host lipid bilayers with different numbers of lipids, as shown in Table 2. A single ULCFA molecule was inserted into the upper leaflet. The system temperature was controlled at 343 K to avoid the gel phase of DSPC and SDPC. The membranes were equilibrated for 200 ns, followed by 800 ns production runs.

(3) We added cholesterols to both the upper and lower leaflets of the bilayer to investigate the effects of cholesterols on the conformation of the ULCFAs. DSPC and SDPC were used as the host lipid molecules. The number of host lipid molecules is 89 in the upper leaflet, and 100 in the lower leaflet. In the initial state, 20 or 40 cholesterols are added in both upper

Table 3: Numbers of lipids in bilayers containing cholesterols. A single dTSPC molecule was embedded.

Membrane	Upper leaflet	Lower leaflet
DS/CHOL20	89 + 20	100 + 20
DS/CHOL40	89 + 40	100 + 40
SD/CHOL20	89 + 20	100 + 20
SD/CHOL40	89 + 40	100 + 40

and lower leaflets, as listed in Table 3. The system temperature was controlled at 343 K to avoid the gel phase of DSPC and SDPC. The DS/CHOL and SD/CHOL mixtures were equilibrated for 1 μs and 3 μs, respectively.

2.3 MD Simulations

The system pressure of all simulations was controlled at 0.101 MPa. The CHARMM 36 force field [24] and TIP3P water model [25] were used to represent lipid and water molecules, respectively. All MD simulations were performed using GROMACS [26].

To calculate the lipid area in the tensionless membranes, we performed MD simulations for a pure symmetric membrane consisting of 100 DSPCs or 100 SDPCs per leaflet. From these MD simulations, we obtained that the area per lipid of DSPC and SDPC are 0.63 and 0.74 nm^2, respectively. Thus, SDPCs have a slightly larger area than DSPCs because of their unsaturated bonds.

3 Results and Discussion

3.1 Conformation of the sn-1 chain of ULCFAs

Figure 3 shows three types of conformations of the sn-1 chain of dTSPC embedded in SD189u bilayer. A turned conformation, in which the C_3-C_{18}-C_{32} angle in the sn-1 chain is approximately 0° is shown in Fig. 3(a). The terminal carbon atom (C_{32}) is located in the upper leaflet. An L-shaped conformation, in which the angle is approximately 90°, is shown in Fig. 3(b). The C_{32} atom is located at the boundary of the two leaflets. An elongated conformation, in which the angle is approximately 180°, is shown in Fig. 3(c). The C_{32} is located in the lower leaflet. The sn-1 chain temporally fluctuates among these conformations. That is, it moves between the upper and lower leaflets and also lies along with the interface between the two leaflets. This conformational fluctuation is rapid, and the transit time between two leaflets is $\sim$ 10 ns. This large conformational fluctuation has not been observed in the other lipids and is specific to ULCFAs. In particular, the elongated conformation penetrates deeply into the opposite leaflet.

These three types of conformations were also observed for dTSPC, HSPC, and LSPC embedded in asymmetric membranes (case 2) under all simulated conditions. Three types of conformations of dTSPC, HSPC, and LSPC are shown in Fig. 4(a), (b), and (c), respectively. The long chain of LSPC is more elongated than that of dTSPC owing to the saturated bonds of the chain.

3.2 Distribution of atoms

The distribution of atoms in the sn-1 chain of ULCFA in a lipid bilayer was calculated along the z-axis, which is parallel to the bilayer normal. The origin of the z-axis is set at the center of the lipid bilayer. Figure 5 shows the probability distribution of C_3, C_{18}, and C_{32} atoms of the sn-1 chain of dTSPC and phosphate (P) atoms of DSPC, SDPC, and SOPC in single-component bilayers (case 1). The terminal carbon C_{32} of the sn-1 chain is widely distributed from z of -2 to 2 nm, corresponding with the conformation fluctuations observed in the snapshots. The free-energy difference $F(z)$ between two conformations were calculated using $F(z) = -k_{\mathrm{B}}T\ln(p(z))$. The estimated value was less than $1.2k_{\mathrm{B}}T$ from $p(z)$ of C_{32}, indicating no apparent free-energy barrier among them.

The distributions of P in DS189u, SD189u,

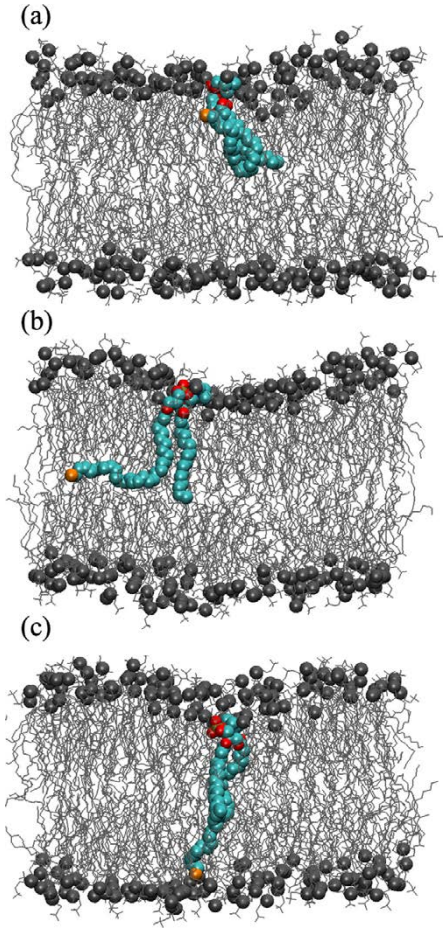

Figure 3: Snapshots of dTSPC in DS189l membrane. (a) Turned conformation. (b) L-shaped conformation. (c) Elongated conformation. dTSPC are represented by colored spheres. Host lipid molecules are shown in gray (spheres represent the phosphate atoms). Water molecules are not shown for clarity.

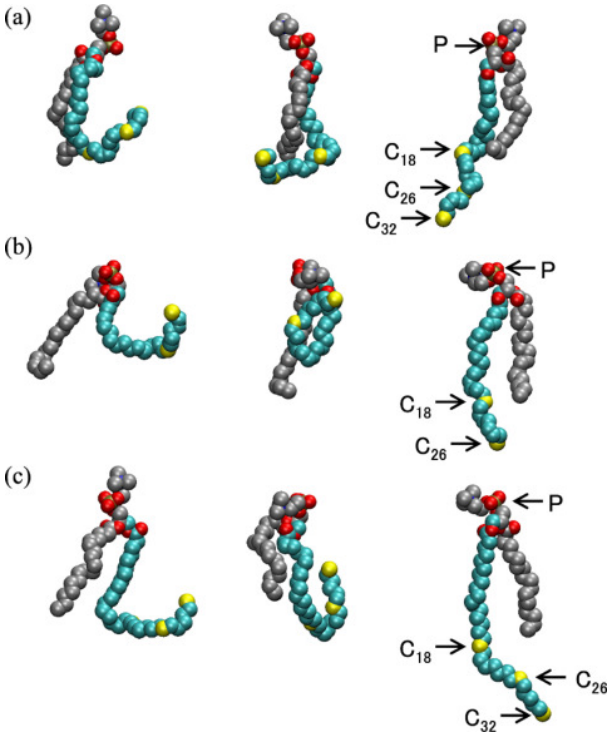

Figure 4: Snapshots of (a) dTSPC, (b) HSPC, and (c) LSPC embedded in lipid bilayers (DS89-SD100). Carbon atoms in the sn-1 chain are shown in cyan and other carbon atoms are shown in gray. Hydrogen atoms are not shown for clarity. Reproduced from Ref. [20].

and SO198u were similar to those in DS189l, SD189l, and SO198l, respectively. as shown in Fig. 5. These results indicate that the membrane thickness does not depend on the lipid-density difference between the two leaflets. Thus, the host lipid bilayer structure is not significantly modified in the examined range of the density difference.

In contrast, the distribution of carbon atoms in the sn-1 chain of dTSPC depends on the lipid-density difference between the two leaflets. As the lipid density relatively decreases in the lower leaflet, the distribution of C_{32} largely shifts toward the lower leaflet. The peak position of C_{18} shifts toward the lower leaflet as observed in C_{32}, but the shift magnitude is smaller. The distribution of C_3 shifts slightly toward the lower leaflet as the lipid density relatively decreases in the lower leaflet. Thus, the longer region ($C_{18} \sim C_{32}$) of the sn-1 chain exhibits larger changes arising from the lipid-density difference between the two leaflets.

To quantitatively investigate the effects of the lipid-density differences on the conformation of the sn-1 chain, we calculated the mean z-position of the C atoms normalized by the mean z-position the P atoms as a function of the lipid density ratio. The lipid density ratio

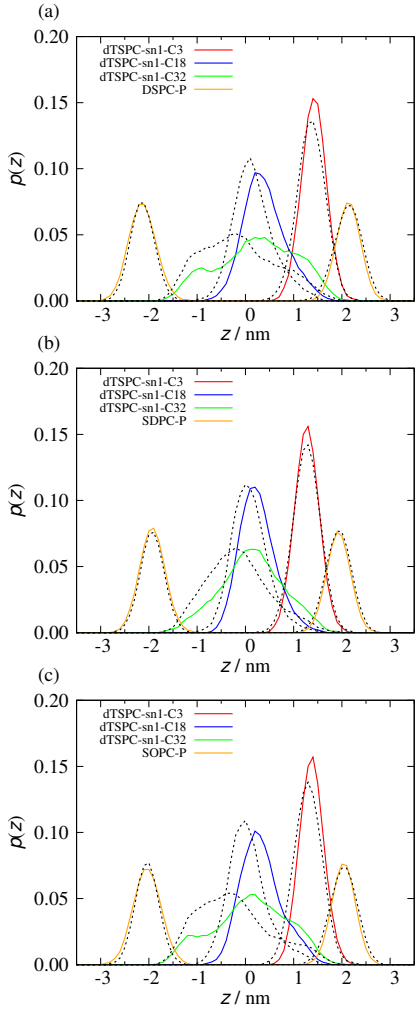

Figure 5: Probability distribution of atoms in (a) DS189u/l, (b) SD189u/l, and (c) SO189u/l systems. The solid and dotted lines represent the probability distributions in 'u' and 'l', respectively. Reproduced from Ref. [19].

is defined as $N_{\rm l}S_{\rm l}/N_{\rm u}S_{\rm u}$, where $N_{\rm l}$ and $N_{\rm u}$ are the numbers of host lipid molecules in the lower and upper leaflets, respectively. $S_{\rm l}$ and $S_{\rm u}$ represent the area per lipid of DSPC or SDPC in the lower and upper leaflets, respectively, obtained from the MD simulations for a pure symmetric membrane.

Figure 6 shows the correlation between the normalized z-position ($z_{\rm C}/z_{\rm P}$) and the lipid density ratio $N_{\rm l}S_{\rm l}/N_{\rm u}S_{\rm u}$ for dTSPC in the DSPC/SDPC asymmetric bilayer (case 2). A positive linear correlation was found between the normalized z-positions of carbon atoms and the lipid density ratio.

From the least-squares fitting (represented by dashed lines), we found that the value of $z_{\rm C}/z_{\rm P}$ was almost 0 for C_{32} at $N_{\rm l}S_{\rm l}/N_{\rm u}S_{\rm u} = 1$. Thus, the terminal carbon is located in the middle of the lipid bilayer in the absence of lipid-density difference and moves to the upper (lower) leaflet as the lipid density of the upper (lower) leaflet decreases. Therefore, the conformational change of the sn-1 chain in dTSPC reduces the lipid-density differences.

In the cases of HSPC and LSPC, we found similar behavior. The ratio of the elongated conformation increases as the lipid density of the opposite leaflet decreases. The position the terminal atom C_{26} of HSPC is almost identical to that of C_{26} in dTSPC. The sn-1 chain of LSPC is more deeply in the lower leaflet than that of dTSPC. We concluded that the reduction of the lipid-density differences between the two leaflets by the change in the ultra-long sn-1 chain conformation is a general property of ULCFAs.

3.3 Order parameters

We calculated the lipid order parameters, $S_{\rm CD}$, using the following equation:

$$S_{\rm CD} = \langle \frac{3\cos^2\alpha - 1}{2} \rangle, \qquad (1)$$

where α is the angle between C-H bond vector and the bilayer normal. The brackets indicate the average over time and lipid molecules. Calculated order parameter profiles, $-S_{\rm CD}$, for ULCFAs embedded in the DS89-SD100 bilayer are shown in Fig. 7. These profiles were not sensitive to lipid-density differences. The order profiles of the sn-1 chain decreased to 0 at C_{15} and exhibited a low order in the longer region until the terminal. The order of the sn-2 chain was similar to that of the sn-2 chain in DSPC, because the sn-2 chain in ULCFAs are equivalent to the sn-2 chain in DSPC. In the case of HSPC, the order profile of the sn-1

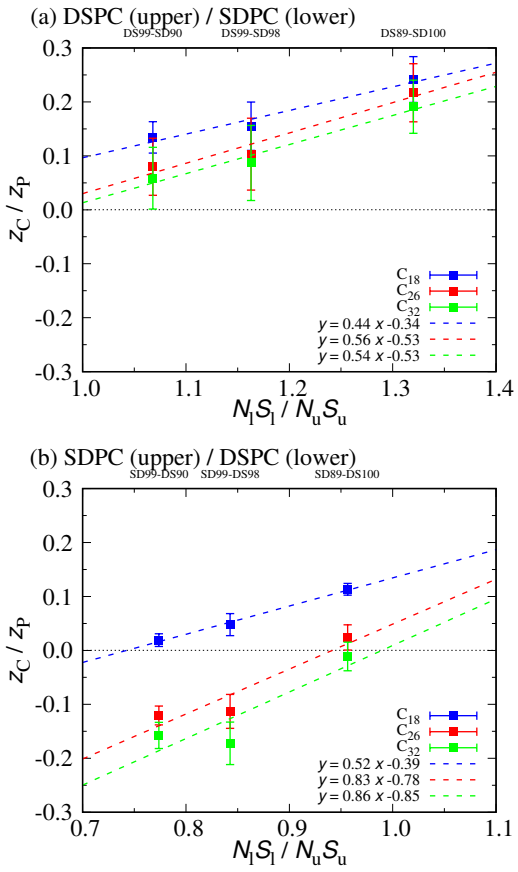

Figure 6: Correlation between normalized z-position of C atoms and lipid-density ratio for dTSPC. Reproduced from Ref. [20].

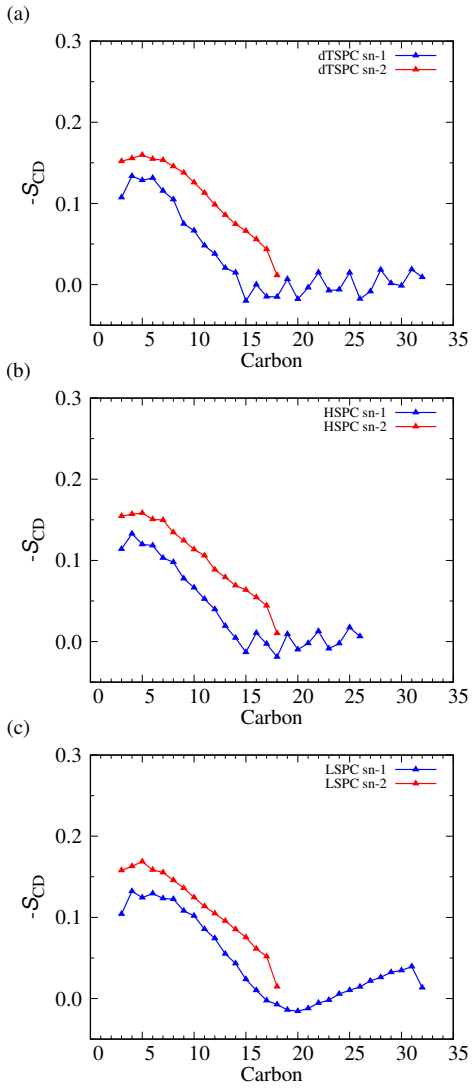

Figure 7: Order parameter profiles, $-S_{CD}$, of (a) dTSPC, (b) HSPC, and (c) LSPC for DS89-SD100. Reproduced from Ref. [20].

chain exhibited a similar profile to that in dTSPC, because the sn-1 chain in HSPC is equivalent to the sn-1 chain until C_{26} in dTSPC. In contrast, the order profile of LSPC becomes higher toward the terminal, because the sn-1 chain of the LSPC has no double bonds. It is indicated that the saturated long chain takes a more elongated conformation than unsaturated long chains.

3.4 dTSPC with Cholesterols

We analyzed the interactions between dTSPC and cholesterols in asymmetric bilayers. Cholesterol molecules were embedded in the asymmetric bilayers with number fractions of 20 % or 40 %, as shown in Table 3. In the initial state of each simulation, the cholesterol fraction in the upper leaflet ($N_{\mathrm{upper}}/N_{\mathrm{total}}$) was set to 0.5.

In the case of the DSPC bilayers, the cholesterol fraction is almost constant (0.5) during 1 μs, showing that the flip–flop time of cholesterols is much longer than 1 μs. On the other hand, in the case of the SDPC bilayers, the fraction frequently changed during 3 μs, showing that the lipid-density difference between the two leaflets was reduced by cholesterols. The flip–flop times per cholesterol molecule were 0.52 and 0.66 μs for SD/CHOL20 and

SD/CHOL40, respectively. These values of flip–flop time are much faster than those of phospholipids (hours or days) but slower than those of ULCFAs. A similar time scale of the cholesterol flip–flop was previously reported in the MD simulations of other lipid compositions [27, 28, 29]. After the cholesterol flip–flop, the conformation distribution of ULCFAs becomes close to that in the absence of the area difference in the two leaflets. Therefore, the area difference is responded by ULCFAs first and later by cholesterols. ULCFAs is a rapid sensor of the area difference.

4 Summary

In this report, we have shown the conformational change of ULCFAs in single-component and asymmetric bilayer membranes using MD simulations. The ultra-long sn-1 chain largely fluctuates between upper and lower leaflets and takes elongated, L-shaped, and turned conformations. ULCFAs can rapidly reduce the lipid-density differences between the two leaflets via the ratio change of these conformations.

References

[1] G. van Meer, D. R. Voelker, and G. W. Feigenson, Nature Rev. Mol. Cell Biol. **9**, 112 (2008).

[2] H. Shindou and T. Shimizu, J. Biol. Chem. **287**, 1 (2009).

[3] B. Anthony, S. Vanni, H. Shindou, and T. Ferreira, Trends Cell Biol. **25**, 427 (2015).

[4] J. P. SanGiovanni and E. Y. Chew, Prog. Retin. Eye Res. **24**, 87 (2005).

[5] A. McMahon and W. Kedzierski, Br. J. Ophthalmol. 1127 (2009).

[6] P. Barabas, A. Liu, W. Xing, C. Chen, Z. Tong, C. B. Watt, B. W. Jones, P. Bernstein, and D. Križaj, Proc. Natl. Acad. Sci. USA **110**, 5181 (2013).

[7] B. Jun, P. K. Mukherjee, A. Asatryan, M. A. Kautzmann, J. Heap, W. C. Gordon, S. Bhattacharjee, R. Yang, N. A. Petasis, N. G. Bazan, Sci. Rep. **7**, 5279 (2017).

[8] F. Deák, R. E. Anderson, J. L. Fessler, D. M. Sherry, Front Cell Neurosci. **13**, 428 (2019).

[9] M. Müller, K. Katsov, and M. Schick, Phys. Rep. **434**, 113 (2006).

[10] M. Venturoli, M. M. Sperotto, M. Kranenburg, and B. Smit, Phys. Rep. **437**, 1 (2006).

[11] H. Noguchi, J. Phys. Soc. Jpn. **78**, 041007 (2009).

[12] R. M. Venable, F. L. H. Brown, and R. W.Pastor, Chem. Phys. Lipids **192**, 60 (2015).

[13] S. J. Marrink, V. Corradi, P. C. T. Souza, H. I. Ingólfsson, D. P. Tieleman and M. S.P. Sansom, Chem. Rev. **119**, 6184 (2019).

[14] A. P. Ramos, P. Lagë, G. Lamoureux, and Michel Lafleur, J. Phys. Chem. B **120**, 6951 (2016).

[15] R. Gupta, B. S. Dwadasi, and B. Rai, J. Phys. Chem. B **120**, 12536 (2016).

[16] T. Róg, A. Orłowski, A. Llorente, T. Skotland, T. Sylvänne, D. Kauhanen, K. Ekroos, K. Sandvig, and I. Vattulainen, Biochim. Biophys. Acta **1858**, 281 (2016).

[17] M. Manna, M. Javanainen, H. M. Monne, H. Gabius, T. Rog, and I. Vattulainen, Biochim. Biophys. Acta **1859**, 870 (2017).

[18] E. Wang and J. B. Klauda, J. Phys. Chem. B **122**, 2757 (2018).

[19] K. Kawaguchi, K. M. Nakagawa, S. Nakagawa, H. Shindou, H. Nagao, and H. Noguchi, J. Chem. Phys. **153**, 165101 (2020).

[20] K. Kawaguchi, H. Nagao, H. Shindou, and H. Noguchi, J. Phys. Chem. B **126**, 9316 (2022).

[21] R. D. Kornberg and H. M. McConnell, Biochemistry **10**, 1111 (1971).

[22] U. Seifert, Adv. Phys. **46**, 13 (1997).

[23] S. Svetina and B. Žekš, Adv. Colloid Interface Sci. **208**, 189 (2014).

[24] J. B. Klauda, I. M. Venable, J. A. Freites, J. W. O'Connor, D. J. Tobias, C. Mondragon-Ramirez, I. Vorobyov, A. D. MacKerell Jr., and R. W. Pastor, J. Phys. Chem. B **114**, 7830 (2010).

[25] A. D. MacKerell Jr. and P. W. Pastor, J. Phys. Chem. B **102**, 3586 (2010).

[26] M. J. Abraham, T. Murtola, R. Schulz, S. Páll, J. C. Smith, B. Hess, and E. Lindahl, SoftwareX **1**, 19 (2015).

[27] S. Jo, H. Rui, J. B. Lim, J. B. Klauda, and W. Im, J. Phys. Chem. B **114**, 13342 (2010).

[28] F. Ogushi, R. Ishitsuka, T. Kobayashi, and Y. Sugita, Chem. Phys. Lett. **522**, 96 (2012).

[29] R. Gu, S. Baoukina, and D. P. Tieleman, J. Chem. Theory Comput. **15**, 2064 (2019).